Preparation of highly polarized nuclei: Observation and control of time-dependent polarization transfer from $H^{35}Cl$ molecular rotation to ^{35}Cl nuclear spin

Dimitris Sofikitis,[1,2] Luis Rubio-Lago,[1] Marion R. Martin,[3] Davida J. Ankeny Brown,[3] Nathaniel C.-M. Bartlett,[3] Richard N. Zare,[3,*] and T. Peter Rakitzis[1,2,†]

[1]*Institute of Electronic Structure and Laser, Foundation for Research and Technology-Hellas, 71110 Heraklion-Crete, Greece*

[2]*Department of Physics, University of Crete, P.O. 2208, 71003 Voutes-Heraklion, Greece*

[3]*Department of Chemistry, Stanford University, Stanford, California 94305-5080, USA*

(Received 20 December 2006; published 11 July 2007)

We demonstrate time-dependent polarization transfer from molecular rotation to nuclear spin. The $H^{35}Cl$ $(v=2, J=1, M=1)$ state is excited with a 1.7 μm laser pulse, and then dissociated with a delayed 235 nm laser pulse to produce ^{35}Cl atoms. Time-dependent polarizations of both $H^{35}Cl$ $(v=2, J=1)$ molecules and $^{35}Cl(^2P_{3/2})$ atoms, which vary due to hyperfine quantum beating, are measured. The ^{35}Cl nuclear spin is highly polarized ($\langle M_{Cl}\rangle \approx 1.1$) at a pump-probe delay of 145 ns. Densities surpassing 10^{14} cm^{-3} are achieved. The technique is applicable to many atoms not amenable to optical pumping.

DOI: 10.1103/PhysRevA.76.012503 PACS number(s): 33.15.Pw, 33.20.Wr, 67.65.+z, 72.25.Fe

Control over angular momentum polarization in atomic and molecular gases is important to many fields, including medical imaging [1], atomic and nuclear collisions [2,3], reaction dynamics [4], and quantum computation [5,6]. Well-established techniques for the preparation of polarized gases such as Stern-Gerlach separation [7] and optical pumping [8] achieve high degrees of atomic polarization (close to 100% for both cases); however, both techniques have major limitations. For example, Stern-Gerlach separation is limited to low densities (typically no more than 10^{12} atoms/cm^3), whereas many atoms do not have efficient optical pumping schemes using existing laser sources. Optical pumping has been applied most successfully with the alkali atoms, and other species can be polarized using the spin-exchange optical pumping technique [3,9]. Recently, the dynamic nuclear polarization (DNP) technique has been developed to produce highly polarized solid and liquid samples [10]. A technique suitable for the preparation of polarized gas-phase atoms at high densities, proposed by van Brunt and Zare [11] but demonstrated only in recent years [12], is molecular photodissociation. This technique is limited by the details of the parent molecule photodissociation mechanism, but many favorable cases have been found. In addition, the dissociation mechanism is only capable of polarizing the electronic angular momentum of the photofragments, leaving any nuclear spin as a source of depolarization. To solve this problem, it was recently proposed to polarize the parent molecules' nuclear spins by transferring polarization from molecular rotation of state-prepared molecules, using the hyperfine coupling interaction [13,14] (a similar proposal was also made for the production of polarized ions [15]). Here, we report the observation of the time-dependent polarization transfer from molecular rotation to nuclear spin, in the case of $H^{35}Cl$ $(v=2, J=1, M=1)$ molecular rotation to ^{35}Cl nuclear spin, on the nanosecond timescale. This work demonstrates a new technique for the production of polarized atoms and molecules, and may be especially useful for the production of polarized atoms and molecules that are not amenable to optical pumping.

The $H^{35}Cl$ $(v=2, J=1, M=1)$ state is prepared at $t=0$ with a laser pulse, without hyperfine resolution. This state corresponds to one quantum of rotational angular momentum that is oriented in the laboratory frame. At later times, polarization is exchanged between the molecular rotation and the ^{35}Cl nuclear spin via the hyperfine quantum beating effect described theoretically elsewhere [11,12,16–18], on a timescale of a few tens of nanoseconds for the case of $H^{35}Cl$. A second laser pulse dissociates the $H^{35}Cl$ $(v=2, J=1)$ state at a later time and thus "freezes" the polarization exchange between the molecular rotation and the ^{35}Cl nuclear spin. Once ^{35}Cl atoms are formed following molecular photodissociation, a similar polarization exchange phenomenon is established between the ^{35}Cl nuclear and electronic angular momentum, only this beating takes place on a much faster, subnanosecond, timescale. This polarization exchange provides an indirect way to probe the nuclear polarization through pulsed-laser detection of the electronic angular momentum polarization, which reflects the original nuclear polarization. Because the Nd-Yag pumped lasers used here have pulse durations of a few nanoseconds, the time-average of the polarization beating between the electronic and the nuclear spin is detected. If the time that elapses between the molecular state-preparation and the photodissociation is gradually increased, then the shape of the quantum beating responsible for the polarization transfer between the molecular rotation and the nuclear spin is observed. Photodissociation and polarization detection can be realized with the same laser pulse, a fact that considerably simplifies our experiment.

A 5% mixture of HCl in He was supersonically expanded into the extraction region of a Wiley-McLaren time-of-flight (TOF) mass spectrometer [shown in Fig. 1(a), and described in detail elsewhere [19]] via a pulsed nozzle operating at 20 Hz (backing pressure between 0.5 and 1 bar), which cools the HCl to a rotational temperature of about 15 K, so that about 60% of the population is in the HCl $(v=0, J=0)$ ground state. This state is subsequently excited to the HCl

*zare@stanford.edu
†ptr@iesl.forth.gr

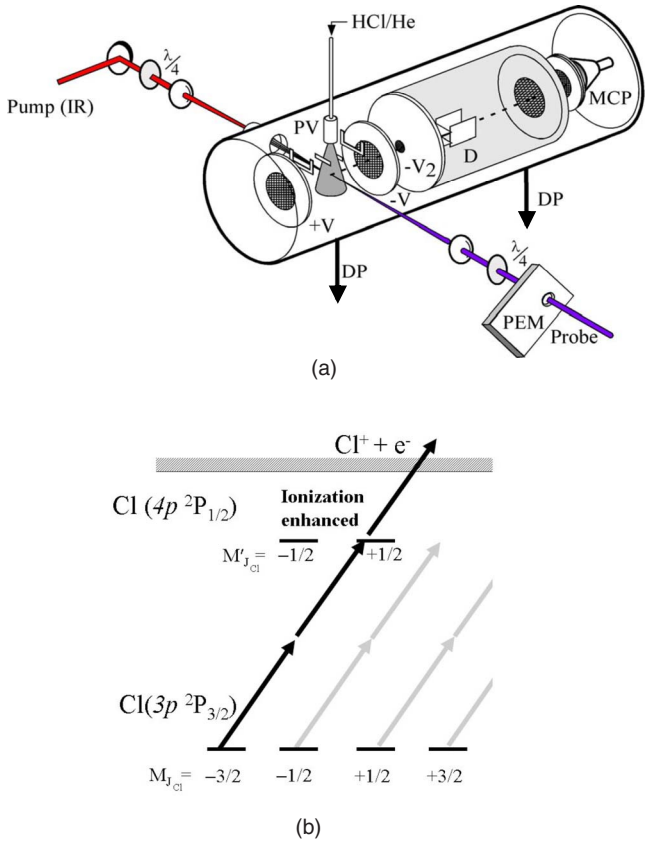

FIG. 1. (Color online) (a) The HCl/He mixture is expanded with a pulsed value (PV) at 20 Hz into the extraction region of the time-of-flight mass spectrometer, and intersected with the circularly-polarized, focused pump and probe laser beams. The extraction and detection regions are pumped with diffusion pumps (DPs) to pressures of about 10^{-5} and 10^{-7} Torr, respectively. Following HCl photodissociation and Cl ionization, the ions are detected with mass and velocity sensitivity with microchannel plates (MCP). (b) Detection of $Cl(^2P_{3/2})$ atoms via 2+1 REMPI using left circularly polarized light at 234.63 nm. *M*-state selection rules and the choice of the intermediate state allows only the $M_{J_{Cl}}=-3/2$ state to be detected for left circularly polarized light.

$(v=2, J=1, M=1)$ state with circularly polarized infrared light at about 1.7 μm [20], such that all the hyperfine states were coherently excited (the laser bandwidth of about 1.0 cm^{-1} is about 1000 times broader than the hyperfine splittings). Approximately 30 mJ/pulse of IR light is generated by a two-step process, involving difference frequency mixing followed by optical parametric amplification [18]. The focused IR light was able to saturated this overtone transition; in contrast, the excitation to HCl $(v=1, J=1)$ can be saturated for a large laser-beam diameter (at least 1 cm), for experiments where a large volume or production rate is required. For the first set of the experiments, HCl $(v=2, J=1)$ molecules were detected by state-specific three-photon ionization at 250.70 nm [21–23]: the molecules are resonantly two-photon excited to the HCl $(v=1, J=2)$ of the electronically excited F state (referred to as the R(1) F-X (1,2) transition), and subsequently one more photon ionizes these excited HCl molecules. The circular polarization was alternated between left and right on a shot-to-shot basis using a photoelastic modulator (PEM 80 Hinds Electronics) and a quarter waveplate to produce ionization signals, denoted by I(L) and I(R). The HCl^+ ions were detected with a TOF mass spectrometer [17] for delays of 0 to 200 ns between the pump (IR) and the probe (UV) laser pulses. For the second set of experiments, $Cl(^2P_{3/2})$ atoms were both produced from the photodissociation of HCl $(v=2, J=1)$ and detected by three-photon ionization via the $4p\ ^2P_{1/2} \leftarrow 3p\ ^2P_{3/2}$ two-photon transition, using circularly polarized light at 234.63 nm [24]. The UV light for the multiphoton-ionization steps is generated by frequency doubling in BBO the output of a Nd:Yag-pumped dye laser, to produce about 2 mJ/pulse [17] (only about 0.1 mJ/pulse was used). Photodissociation of HCl occurs via the $A\ ^1\Pi(1)$, $a^3\Pi(1)$, and $t^3\Sigma(1)$ states to produce $Cl(^2P_{3/2})$ and $Cl(^2P_{3/2})$ atoms [25]; the latter, if probed, should also show similar polarization effects. As before, the I(L) and I(R) signals were detected for pump-probe delays between 0 to 200 ns. In Fig. 1(b) we show the ionization scheme of the $Cl(^2P_{3/2})$ atoms, demonstrating that only the $M_{J_{Cl}}=-3/2$ state is detected for I(L), and only the $M_{J_{Cl}}=+3/2$ state for I(R). We note that our experimental scheme is only sensitive to polarization produced by the infrared pump laser, and not to any electronic Cl-atom polarization produced by the photodissociation, as the photodissociation and probe steps occur with the same laser pulse, so that the relative polarizations of the photodissociation and probe photons is the same for I(L) and I(R).

In Fig. 2 we display the signal ratio $R=[I(L)-I(R)]/[I(L)+I(R)]$ for the detection of the HCl $(v=2, J=1)$ state and $Cl(^2P_{3/2})$ atoms, as well as the theoretical predictions for this ratio, for pump-probe delays between 0 and 200 ns. These signals can be expressed in the form of a multipole expansion,

$$I(R) = I_0[1 + s_1 A_0^{(1)}(J_{HCl}, t=0) G^{(1)}(t) + s_2 A_0^{(2)}(J_{HCl}, t=0) G^{(2)}(t)], \quad (1a)$$

$$I(L) = I_0[1 - s_1 A_0^{(1)}(J_{HCl}, t=0) G^{(1)}(t) + s_2 A_0^{(2)}(J_{HCl}, t=0) G^{(2)}(t)], \quad (1b)$$

where the $A_0^{(k)}(J_{HCl}, t=0)$ describe the initial m-state distribution of the $HCl(v=2, J=1)$ state: $A_0^{(1)}(J_{HCl}, t=0)=1/\sqrt{2}$ and $A_0^{(2)}(J_{HCl}, t=0)=1/2$, which give $p(J_{HCl}=1, M_{J_{HCl}}=1)=1$ and $p(J_{HCl}=1, M_{J_{HCl}}\neq 1)=0$ at $t=0$ [11]. The $G^{(k)}(t)$ give the time-dependence of the *M*-state distribution due to the hyperfine beating [11], and the s_k are the detection sensitivity factors for the $A_0^{(k)}$ parameters in the ionization scheme; for the R(1) F-X (1,2) transition used here, $s_1=-1/\sqrt{2}$ and $s_2=-1$. Notice that the only difference between I(R) and I(L) is the sign of the dipole term $(k=1)$, which is sensitive to the helicity of the probe light. Equation (1) is used to calculate the signal ratio $R=[I(L)-I(R)]/[I(L)+I(R)]$ shown in Fig. 2(a).

In Fig. 2(b) we similarly display the ratio R for $Cl(^2P_{3/2})$ atoms as well as the theoretical prediction. The time-

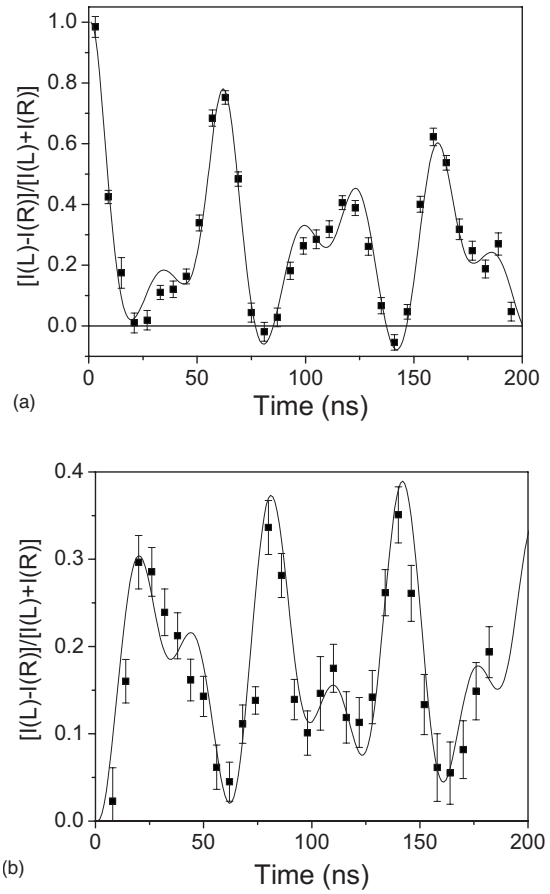

FIG. 2. The signal ratio R=[I(L)−I(R)]/[I(L)+I(R)] as a function of pump-probe time delay using left (L) and right (R) circularly polarized probe light for (a) HCl ($v=2, J=1$) molecules detected at 250.70 nm, and (b) Cl($^2P_{3/2}$) atoms detected at 234.63 nm. Data are plotted along with theoretical predictions in both cases (see text). The error bars are 2σ.

dependence of the Cl-atom ionization signals can also be described by a multipole expansion,

$$\mathrm{I(R)} = I_0[1 + s_1 H_{\mathrm{av}}^{(1)} A_0^{(1)}(I_{\mathrm{Cl}}, t=0) H^{(1)}(t) + s_2 H_{\mathrm{av}}^{(2)} A_0^{(2)}(I_{\mathrm{Cl}}, t=0) H^{(2)}(t)], \quad (2a)$$

$$\mathrm{I(L)} = I_0[1 - s_1 H_{\mathrm{av}}^{(1)} A_0^{(1)}(I_{\mathrm{Cl}}, t=0) H^{(1)}(t) + s_2 H_{\mathrm{av}}^{(2)} A_0^{(2)}(I_{\mathrm{Cl}}, t=0) H^{(2)}(t)], \quad (2b)$$

where $s_1=9/\sqrt{15}$ and $s_2=5/4$ for the detection transition of the Cl($^2P_{3/2}$) atoms. The $H_{\mathrm{av}}^{(k)}$ factors, equal to $G_{\mathrm{av}}^{(k)}$, describe the time-averaged degree of the polarization of the electronic spin, which has been transferred from the ^{35}Cl nuclear spin polarization; here $H_{\mathrm{av}}^{(1)}=0.5$ and $H_{\mathrm{av}}^{(2)}=0.27$ [15].

In Fig. 3 we display the time-dependent M-state expectation values $\langle M_{J_{\mathrm{HCl}}}(t)\rangle$ and $\langle M_{I_{\mathrm{Cl}}}(t)\rangle$, by multiplying the polarization data for the HCl ($v=2, J=1$) molecule and the Cl($^2P_{3/2}$) atom by the factor I(L)+I(R) from Eqs. (1) and (2), respectively. The Cl($^2P_{3/2}$) atom data is multiplied by an extra factor of 2 to show the nascent ^{35}Cl nuclear polarization, as the polarization is later shared equally between the nuclear

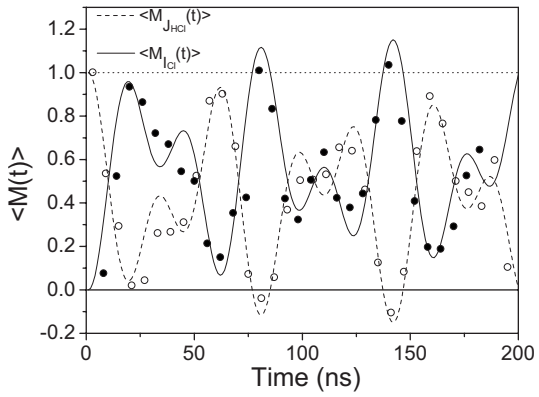

FIG. 3. Plots of the time-dependent m-state expectation values $\langle M_{J_{\mathrm{HCl}}}(t)\rangle$ and $\langle M_{I_{\mathrm{Cl}}}(t)\rangle$ for the HCL ($v=2, J=1$) state (open circles) and the Cl($^2P_{3/2}$) atoms (solid circles), produced by transforming the raw data from Fig. 2 (see text). Theoretical predictions correspond to the $\langle M_{J_{\mathrm{HCl}}}(t)\rangle = G^{(1)}(t)$ (dashed line) and $\langle M_{I_{\mathrm{Cl}}}(t)\rangle = \sqrt{15/8}H^{(1)}(t)$ (solid line) polarization factors. Notice that $\langle M_{J_{\mathrm{HCl}}}(t)\rangle + \langle M_{I_{\mathrm{Cl}}}(t)\rangle = 1$ (dotted line), showing the conservation of angular momentum projection.

and electronic angular momentum. We see that the values of $\langle M_{J_{\mathrm{HCl}}}(t)\rangle$ and $\langle M_{I_{\mathrm{Cl}}}(t)\rangle$ vary in a complementary fashion and sum to unity, as expected from conservation of angular momentum projection (and the fact that polarization transfer to the proton spin is negligible on these timescales). For a pump-probe delay of 145 ns, the ^{35}Cl nuclear polarization reaches a maximum value of $\langle M_{I_{\mathrm{Cl}}}(t)\rangle \approx 1.1$, when $\langle M_{J_{\mathrm{HCl}}}(t)\rangle \approx -0.1$. The agreement between the experimental measurement and the theoretical prediction matches within experimental error, and we see no depolarization on these timescales and under these experimental conditions. We are not aware of the depolarization rates of the polarized Cl($^2P_{3/2}$) atoms, so we cannot estimate the polarization dependence at longer times than observed here.

In these experiments, the supersonic expansion produces an HCl density of about 10^{15} cm^{-3} at the laser interaction region. About 30% of these molecules (within the IR beam) are excited to the HCl ($v=2, J=1$) state and, subsequently, approximately all of them can be photodissociated (within the tightly focussed UV beam), so that the pulsed Cl atom density in this small region is about 10^{14} cm^{-3}, with production rates about 10^{11}/pulse. These densities and rates can be increased significantly (up to about 2 and 4 orders of magnitude, respectively) with higher HCl densities in the expansion, and with a larger pump-probe laser volume [achieved with higher photodissociation-laser power and/or with multiple passes of the photodissociation laser beam, and IR pumping the HCl ($v=1, J=1$) state, allowing a large IR beam].

The resulting polarized atoms, with fixed speeds from the recoil of the photodissociation, can be used to study spin-dependent collisions with other target atoms or molecules in the beam, using the well-established photoloc technique [17], for which the collisions are initiated by the recoil speed of the polarized photofragments. For cases where the polarized atoms are used as a stationary polarized target, a disadvan-

tage of this technique is that the polarized photofragments may need to be separated from the unphotodissociated parent molecules, which may constitute an unpolarized background that cannot be separated from the desired signal. In this case, the parent molecule can be prepared in a skimmed molecular beam, so that upon photodissociation or dissociative ionization the polarized atoms or ions can recoil beyond the molecular beam, where they can be collided with other targets, including electron or ion beams [26], or with a surface [27], or the spin orientation can be used to measure nuclear properties such as nuclear moments or directed particle emissions from radioactive decay [28–30]. This separation procedure will lower the polarized atom density by at least an order of magnitude, but it still remains high enough for many potential applications.

Polarization transfer from the molecular rotation to the nuclear spin can be considered as a new and independent method for the preparation of highly polarized atomic or molecular gases. If the electronic angular momentum is also highly polarized by the photodissociation process itself, something that has been proved to happen when the photodissociation light is circularly polarized and the dissociation dynamics appropriately chosen [31], the polarization transfer between the electronic and the nuclear spin can be limited or completely stopped because both these angular momenta will be highly polarized. A combination of these two techniques can lead to the preparation of atomic gases with both the electronic and the nuclear spin highly polarized and at densities close to the parent molecule. Advantages of these techniques include production of polarized atoms on nanosecond timescales at much higher pulsed-densities than current techniques (as high as 10^{16} atoms/cm^3) for atomic systems that cannot be produced using optical pumping, such as the case of polarized $^{35}Cl(^2P_{3/2})$ atoms demonstrated here.

ACKNOWLEDGMENTS

We gratefully acknowledge support from the G.S.R.T. Bilateral Collaboration grant Greece-U.S.A. (05NON-EU-68), the European Commission transfer of knowledge grant Southern Dynamics MTKD-CT-2004-014306, and the U.S. National Science Foundation Grant No. 0242103.

[1] M. S. Albert *et al.*, Nature (London) **370**, 199 (1994).
[2] E. Steffens and W. Haeberli, Rep. Prog. Phys. **66**, 1887 (2003).
[3] S. G. Redsun, R. J. Knize, G. D. Cates, and W. Happer, Phys. Rev. A **42**, 1293 (1990).
[4] R. D. Levine, *Molecular Reaction Dynamics* (Cambridge University Press, Cambridge, 2005).
[5] N. Gershenfeld and I. L. Chuang, Science **275**, 350 (1997).
[6] M. Steffen, L. M. K. Vandersypen, and I. L. Chuang, IEEE Microw. Mag. **21**, 24 (2001).
[7] K. Zapfe *et al.*, Rev. Sci. Instrum. **66**, 28 (1995).
[8] W. Happer, Rev. Mod. Phys. **44**, 169 (1972).
[9] T. G. Walker, W. Happer, Rev. Mod. Phys. **69**, 629 (1997).
[10] J. H. Ardenkjaer-Larsen *et al.*, PNAS **100**, 10158 (2003).
[11] R. J. van Brunt and R. N. Zare, J. Chem. Phys. **48**, 4304 (1968).
[12] T. P. Rakitzis, ChemPhysChem **5**, 1489 (2004), and references therein.
[13] T. P. Rakitzis, Phys. Rev. Lett. **94**, 083005 (2005).
[14] L. Rubio-Lago, D. Sofikitis, A. Koubenakis, and T. P. Rakitzis, Phys. Rev. A **74**, 042503 (2006).
[15] T. Nakajima, Appl. Phys. Lett. **84**, 3786 (2004).
[16] K. Blum, *Density Matrix Theory and Applications* (Plenum Press, New York, 1981).
[17] R. N. Zare, *Angular Momentum* (Wiley, New York, 1988).
[18] R. Altkorn, R. N. Zare, C. H. Greene, Mol. Phys. **55**, 1 (1985).
[19] W. R. Simpson, T. P. Rakitzis, S. A. Kandel, A. J. Orr-Ewing, and R. N. Zare, J. Chem. Phys. **103**, 7313 (1995).
[20] J. P. Camden *et al.*, J. Phys. Chem. A **108**, 7806 (2004).
[21] A. Yokoyama and T. Takayanagi, Chem. Phys. Lett. **302**, 48 (1999).
[22] A. J. Orr-Ewing, W. R. Simpson, T. P. Rakitzis, and R. N. Zare, Isr. J. Chem. **34**, 95 (1994).
[23] H. Lammer, R. T. Carter, and J. R. Huber, Eur. Phys. J. D **8**, 385 (2000).
[24] NIST, 2006. Atomic spectra database, http://physics.nist.gov/PhysRefData/ASD/index.html
[25] P. M. Regan, D. Ascenzi, A. Brown, G. G. Balint-Kurti, and A. J. Orr-Ewing, J. Chem. Phys. **112**, 10259 (2000).
[26] A. Deshpande, R. Milner, R. Venugopalan, and W. Vogelsang, Annu. Rev. Nucl. Part. Sci. **55**, 165 (2005).
[27] Y. Ikedo, Y. Sueyoshi, T. Shimizu, E. Hirose, H. Hori, and E. Torikai, Surf. Interface Anal. **37**, 197 (2005).
[28] K. Asahi *et al.*, Hyperfine Interact. **136**, 183 (2001).
[29] N. J. Stone, J. Rikovska, Sun Punan, and A Woehr, Hyperfine Interact. **136**, 183 (2001).
[30] D. H. Chaplin and W. D. Hutchison, Hyperfine Interact. **136**, 239 (2001).
[31] T. P. Rakitzis *et al.*, Science **300**, 1936 (2003).